REVISTA INTERDISCIPLINAR DE PESQUISA EM ENGENHARIA

CILAMCE 2016

XXXVII IBERIAN LATIN AMERICAN CONGRESS ON COMPUTATIONAL METHODS IN ENGINEERING
BRASÍLIA - DF - BRAZIL

A HYBRIDIZED CONTINUOUS/DISCONTINUOUS GALERKIN FORMULATION FOR STOKES PROBLEM WITH CONTINUOUS TRACE SPACE

Katia P. Fernandes

katiapf1@yahoo.com.br

Webe João Mansur

webe@coc.ufrj.br

Civil Engineering Department, COPPE, PEC, LAMEMO, Federal University of Rio de Janeiro

Av. Pedro Calmon s/n, Ilha do Fundão, 21945-970, P.B. 68506, Rio de Janeiro, RJ, Brazil

Eduardo G.D. do Carmo

carmo@con.ufrj.br

Nuclear Engineering Department, COPPE, Federal University of Rio de Janeiro

Av. Pedro Calmon s/n, Ilha do Fundão, 21945-970, P.B. 68509, Rio de Janeiro, RJ, Brazil

Abstract. *In this paper is presented a new hybridized continuous / discontinuous Galerkin formulation via continuous trace space for the Stokes problem. The method possesses unique features which distinguish itself from other methods. One of these features is that all the discontinuous variables are eliminated at element level as function of continuous trace variable, reducing thus the number of degrees of freedom and consequently the global system. Continuity and weak coercivity are presented in a suitable norm for the proposed formulation. Error estimates are also well established for velocity and pressure. Numerical experiments with the problem having smooth solution confirm the error estimates as well as the robustness of the formulation presented in this paper. Also, the numerical experiments with the classical cavity problem showed that the method presented here possesses a good ability for capturing the singularities of the pressure on the corners.*

Keywords: *Hybrid methods, Discontinuous Galerkin methods, Stokes problem*

1 INTRODUCTION

Discontinuous Galerkin (DG) methods have been used to solve a wide variety of problems, including structural mechanics, fluid mechanics, electromagnetic, among others. Discontinuous Galerkin methods are closely related for using broken function spaces. Important contributions, mainly involving fluids, have shown advantages over continuous Galerkin (CG) methods are presented in Arnold et al. (2001); Baumann & Oden (1999); do Carmo & Duarte (2000); Reed & Hill (1973). The main property of DG methods is to allow a better compatibility between the spaces of velocity and pressure, but this is only possible if the problem is formulated in the element level and the continuity is being weakly imposed between the elements. However, it is important to mention that the DG methods are more costly than the usual CG formulation, because they introduce a significant increase in the degrees of freedom of the problem.

Based on the better properties of classical discontinuous Galerkin methods, new discontinuous Galerkin formulations have been developed to preserve the main properties of classical Galerkin discontinuous methods, as well as, through appropriate static condensation at the element level, reduce the number of degrees of freedom to the same order as the usual continuous Galerkin formulations. Hughes et al. (2006) is the pioneering work in the construction of a new discontinuous Galerkin formulation with these properties. This formulation is based on a kind of continuous / discontinuous formulation, with the discontinuous component being eliminated at the element level in terms of the continuous component. Hybridized discontinuous Galerkin (HDG) methods presented in Cockburn et al. (2005); Nguyen et al. (2010); Cockburn et al. (2011); Egger & Waluga (2013) also preserve these properties. In these formulations, the trace spaces are continuous in the interior of edges or faces, but discontinuous on the boundary of edges or faces.

Recently, motivated by do Carmo et al. (2014), a new hybridized continuous / discontinuous Galerkin formulation with the trace space being continuous was developed for the Stokes problem. In the proposed formulation, all the discontinuous variables are eliminated at element level as function of continuous trace variable. Thereby, the number of degrees of freedom is reduced, which generates a smaller global system than the usual hybridized formulation and the CG formulation.

The paper is organized as follows. In Section 2, we introduce the Stokes problem. The hybridized continuous / discontinuous formulation associated to the model problem is presented in Section 3. Consistency analysis and an analysis of the continuity and weak coercivity in an adequate norm are presented in Section 4. Moreover, an error estimates are also well established for velocity and pressure. Numerical results are presented in Section 5 in order to to verify the robustness and accuracy of the proposed formulation. Finally, in Section 6 we present some conclusions and remarks.

2 THE STOKES PROBLEM

Let $\Omega \subset \mathbb{R}^N (N \in \{2,3\})$ be an open bounded domain having Lipschitz continuous smooth piecewise boundary denoted by Γ. The model problem consists of finding $(\mathbf{u}, p) \in$

$([H^1_{div}(\Omega)]^N \times (H^1(\Omega) \cap L^2_0(\Omega)))$ such that

$$\left\{ \begin{array}{rcl} -div(G\nabla \mathbf{u}) + \nabla p &=& \mathbf{f} \quad \text{and} \quad div(\mathbf{u}) = 0 \quad \text{a.e. in } \Omega, \\ \mathbf{u} &=& \mathbf{g} \quad \text{on } \Gamma, \end{array} \right. \tag{1}$$

where $[H^1_{div}(\Omega)]^N = \{\mathbf{u} \in [H^1(\Omega)]^N;\ div(G\nabla\mathbf{u}) \in L^2(\Omega)\}$, $\mathbf{f} \in [L^2(\Omega)]^N$, $\mathbf{u}$ denotes the velocity field, p denotes the pressure, $\mathbf{g} \in [H^{1/2}(\Gamma)]^N \cap [C^0(\Gamma)]^N$, the spaces $H^{1/2}(\Gamma)$, $C^0(\Gamma)$, $L^2(\Omega)$, $H^1(\Omega)$ as well as the respective product spaces $[H^{1/2}(\Gamma)]^N$, $[C^0(\Gamma)]^N$, $[L^2(\Omega)]^N$ and $[H^1(\Omega)]^N$ are as defined in Adams (1975) and the space $L^2_0(\Omega) = \{v \in L^2(\Omega);\quad \int_\Omega v d\Omega = 0\}$.

Consider $G \in H^1(\Omega) \cap C^0(\Omega \cup \Gamma)$ and satisfying $0 < G_0 \leq G \leq \bar{G}$ in Ω, where G_0 and $\bar{G}$ are positive real constants. Here, G is the dynamic viscosity. Moreover, it is assumed $\mathbf{g}$ satisfying the compatibility condition $\int_\Gamma \mathbf{g} \cdot \mathbf{n} d\Gamma = 0$, where $\mathbf{n}$ is the outward normal unit vector defined almost everywhere on Γ.

Henceforth, we consider $\mathbf{x} \cdot \mathbf{y}$ as being the usual scalar product between two vectors $\mathbf{x}$ and $\mathbf{y}$ belonging to $\mathbb{R}^m$ ($m > 1$ being an integer) as well as $\mathbf{A} \cdot \mathbf{B}$ the usual scalar product between two arbitrary matrices $\mathbf{A}$ and $\mathbf{B}$ of order $n \times m$ ($n > 1$ being an integer) and $\|\circ\|$ the Euclidean norm.

3 THE HYBRIDIZED CONTINUOUS / DISCONTINUOUS GALERKIN FORMULATION VIA TRACE SPACE

In this section we will obtain a hybridized continuous / discontinuous Galerkin formulation via trace space for the problem presented in (1). However, firstly, we need to introduce the set $M^h = \{\Omega_1, \ldots, \Omega_{N_e}\}$ formed by non degenerate finite elements Ω_i ($i = 1, \ldots, N_e$), with M^h being a partition of domain $\Omega \subset \mathbb{R}^N (N \in \{2, 3\})$, satisfying the conditions imposed by the finite element methods. As defined in Ern & Guermond (2004) this partition is quasi regular, such that the constants of inverse estimates only depend on the polynomial degree, i.e. being independent of the mesh parameters. We also consider that the diameter of Ω_i and its boundary are denoted by h_i and Γ_i, respectively. Also, for any function F, defined in Ω, we denote by F_i its restriction to Ω_i. Moreover, we assume that $G_i \in C^\infty(\Omega_i \cup \Gamma_i)$, where G_i is the usual restriction of G to Ω_i. We define the following sets

$$\begin{array}{l} \mathcal{E}^h = \{e; e \text{ is an face of element } \Omega_i\ ; \forall \Omega_i \in M^h\}, \quad \mathcal{E}^{h,0} = \{e \in \mathcal{E}^h;\ e \subset \Omega\}, \\ \Gamma_{i,e} = \Gamma_i \cap e,\ \forall e \in \mathcal{E}^h, \quad \Gamma_{int} = \bigcup_i \Gamma_{i,int} \quad \text{and} \quad \Gamma_{i,int} = \bigcup_{e \in \mathcal{E}^{h,0}} \Gamma_{i,e}. \end{array} \tag{2}$$

For each pair Ω_i and Ω_j such that $\Gamma_i \cap \Gamma_j = e$ where $e \in \mathcal{E}^{h,0}$, we define the new mesh parameters associated to the faces of the elements $h_{i,e} = h_{j,e} = \inf\{h_i, h_j\}$. Also, for each $l \geq 0$ being an integer, consider $P^l(\Omega_i)$ as being the space of polynomials of degree less or equal to l in the local coordinates that define the standard element associated to Ω_i.

For each $p \in L^2(\Omega)$ we consider that its restriction to Ω_i is decomposed by $p_i = \hat{p}_i + \overline{p}_i$, where $\hat{p}_i$ denotes the null average component of p_i and $\overline{p}_i$ the constant component of pressure.

With the goal of stabilizing the constant component of the pressure at the element level, a continuous space of approximation of the velocity must have shape functions which assume non-zero value at the center of one face and zero in the other faces. This should happen for all faces, as mentioned in Fortin (1981). For example, the condition is satisfied using polynomial functions with $l \geq 2$ for the case $N = 2$. Thus, we can introduce the local space, for the case $(N = 2)$ and $l \geq l_0^* = 2$ as $P^{l,*}(\Omega_i) = P^l(\Omega_i)$. The local space for $N = 3$ can be found in do Carmo et al. (submitted).

Our next step is to define the approximation spaces for the velocity and pressure fields and the trace space as follow

$$\begin{aligned} H^{h,k_v,N} &= \{\mathbf{v} \in [L^2(\Omega)]^N;\ \mathbf{v}_i \in [P^{k_v,*}(\Omega_i)]^N\} \quad (k_v \geq l_o^*), \\ P^{h,k_p} &= \{q \in E_0^{1,p};\ q_i \in P^{k_p}(\Omega_i)\}\ (k_p \geq 0), \\ E_0^{1,p} &= \{q \in L_0^2(\Omega); q_i \in H^1(\Omega_i)\}, \\ T^{h,k_t,N} &= \{\mathbf{r} \in [C^0(\Gamma \cup \Gamma_{int})]^N \text{ with } \mathbf{r} \text{ in } \Gamma_i \text{ being the trace} \\ &\quad \text{of an element of } [P^{k_t,*}(\Omega_i)]^N \text{ on } \Gamma_i\} \quad (k_t \geq l_o^*). \end{aligned} \tag{3}$$

The spaces defined in (3) will be used to define the bilinear forms to stabilize the component of null mean. One of the main differences of our formulation in relation to the usual hybridized methods is the definition of the space $T^{h,k_t,N}$, which is formed by continuous functions on $(\Gamma \cup \Gamma_{int})$.

Now, we need to introduce the appropriate bilinear forms for stabilizing the null average component, for any value of $k_p \geq 0$, for any degree of refinement and independent of the mesh be affine or not. With this goal, we consider the projection operator $Q^i_{proj}(\circ)$, which is defined from $P^{k_p}(\Omega_i)$ into $[P^{k_v}(\Omega_i)]^N$ and given by the variational problem: Find, for each $p \in P^{k_p}(\Omega_i)$, the element $\mathbf{Q}^i_{proj}(p) \in [P^{k_v}(\Omega_i)]^N$ that satisfies the following variational equation

$$\int_{\Omega_i} \mathbf{Q}^i_{proj}(p) \cdot \mathbf{v} d\Omega = \int_{\Omega_i} \nabla p \cdot \mathbf{v} d\Omega \quad \forall \mathbf{v} \in [P^{k_v}(\Omega_i)]^N. \tag{4}$$

If the mesh is affine and $k_v \geq (k_p - 1)$, then $\mathbf{Q}^i_{proj}(p) = \nabla p,\ \forall p \in P^{k_v}(\Omega_i)$, therefore, the null average component of the pressure is stabilized. However, we lose the property above if the mesh is not affine or $k_v < (k_p - 1)$.

To obtain a bilinear form to stabilize the null average component of the pressure at element level, it is necessary to use the inequality

$$\|\nabla p_i\|^2 \leq 2\left[\left\|\mathbf{Q}^i_{proj}(p)\right\|^2 + \left\|\mathbf{Q}^i_{proj}(p) - \nabla p_i\right\|^2\right], \quad \forall \Omega_i. \tag{5}$$

The second term of the inequality given in (5) suggests that if the variational formulation has the bilinear form of projection defined by

$$a^{h,i}_{proj}(p,q) = \frac{\rho_{i,1}}{\overline{G_i}}(h_i)^2 \int_{\Omega_i} (\mathbf{Q}^i_{proj}(p) - \nabla p) \cdot (\mathbf{Q}^i_{proj}(q) - \nabla q) d\Omega, \quad \forall (p,q) \in [P^{h,k_p}]^2, \tag{6}$$

then this bilinear form, together with the variational problem given in (4), can stabilize the null average component of the pressure if the mesh is affine or not for any $k_p \geq 0$. In Eq. (6), $\rho_{i,1} > 0$ is a real constant and $\overline{G_i}$ is the average value of G_i in Ω_i.

Note that, to introduce this bilinear form we need to introduce the term not consistent $\int_{\Omega_i} \left\|\mathbf{Q}^i_{proj}(p) - \nabla p\right\|^2 d\Omega$. Following that, an error estimate for this term must be presented. This error estimate is given by the following proposition.

Proposition 1. *Consider $k_{vp} = \inf\{k_v, k_p\}$. If the mesh satisfies the shape-regular condition according to Ern & Guermond (2004), then for each $\Omega_i (i \in \{1, \ldots, N_e\})$, there exists a real constant $C_i^{P,0} > 0$ that is independent of the mesh parameters but possibly dependent of k_{vp}, such that $\forall p \in P^{h,k_p}$ we have the following inequality*

$$\begin{aligned} \sum_{i=1}^{N_e} \int_{\Omega_i} \frac{\rho_{i,1}}{\overline{G}_i} (h_i)^2 \left\| \mathbf{Q}^i_{proj}(p_i) - \nabla p_i \right\|^2 d\Omega \ &\leq \ \sum_{i=1}^{N_e} N C_i^{P,0} \frac{\rho_{i,1}}{\overline{G}_i} (h_i)^{2(k_{vp}+1)} \\ &\times \ (\|p_i\|_{H^{(k_{vp}+1)}(\Omega_i)})^2. \end{aligned} \tag{7}$$

Proof. Let p be an arbitrary element of P^{h,k_p}. For any $s \in P^{k_p}(\Omega_i)$, the element $\boldsymbol{\omega}_i = \mathbf{Q}^i_{proj}(s) - \nabla s + \nabla s - \mathbf{v}_i$ is also an element of $[P^{k_v,*}(\Omega_i)]^N$, $\forall \mathbf{v}_i \in [P^{k_v,*}(\Omega_i)]^N$. Using this fact and the variational Eq. (4) together with the Cauchy-Schwartz inequality, we obtain $\forall \mathbf{v}_i \in [P^{k_v,*}(\Omega_i)]^N$ the inequality

$$\sum_{i=1}^{N_e} \int_{\Omega_i} \frac{\rho_{i,1}}{\overline{G}_i} (h_i)^2 \left\| \mathbf{Q}^i_{proj}(s) - \nabla s \right\|^2 d\Omega \leq \sum_{i=1}^{N_e} \int_{\Omega_i} \frac{\rho_{i,1}}{\overline{G}_i} (h_i)^2 (\|\nabla s - \mathbf{v}_i\|)^2. \tag{8}$$

Based on the usual inverse estimates and using the fact that the space $P^{k_{vp}}(\Omega_i)$ has finite dimension, we can obtain $\forall r \in P^{k_{vp}}(\Omega_i)$ the inequality

$$(h_i)^2 \left(\|\nabla r\|_{[H^{k_{vp}+1}(\Omega_i)]^N} \right)^2 \leq C_i^{inv,k_{vp}} \left(\|r\|_{[H^{k_{vp}}(\Omega_i)]^N} \right)^2, \ \forall r \in P^{k_{vp}}(\Omega_i). \tag{9}$$

From the properties of approximation of $H^{h,k_v,N}$, we can find $\mathbf{v}^{h,p} \in H^{h,k_v,N}$ such that

$$\begin{aligned} &\sum_{i=1}^{N_e} \int_{\Omega_i} \frac{\rho_{i,1}}{\overline{G}_i} (h_i)^2 \left\| \nabla p_i - \mathbf{v}^{h,p} \right\|^2 d\Omega \leq \sum_{i=1}^{N_e} C_i^{P,0,0} \frac{\rho_{i,1}}{\overline{G}_i} (h_i)^2 (h_i)^{2(k_{vp}+1)} \\ &\times \left(\|\nabla p_i\|_{[H^{k_{vp}+1}(\Omega_i)]^N} \right)^2 \leq \sum_{i=1}^{N_e} N C_i^{P,0,0} C_i^{inv,k_{vp}} \frac{\rho_{i,1}}{\overline{G}_i} (h_i)^{2(k_{vp}+1)} \\ &\times \left(\|p_i\|_{[H^{k_{vp}+1}(\Omega_i)]^N} \right)^2. \end{aligned} \tag{10}$$

By defining the constant $C_i^{P,0} = C_i^{P,0,0} C_i^{inv,k_{vp}}$ the result follows immediately from (8) and (10). □

Our formulation possesses another unique property which eliminates the discontinuous components in function of the trace variable that are completely continuous. As a consequence, we have a full static condensation of pressure at the element level. We now define a penalty bilinear form, at element level, only for the constant component of pressure as follows

$$\overline{b}^i_p(q, r) = \int_{\Omega_i} \frac{\lambda^* (h_i)^\lambda}{\overline{G}_i} \overline{q}_i \overline{r}_i d\Omega \quad \text{with} \quad \overline{q}_i = \frac{\int_{\Omega_i} q_i d\Omega}{\int_{\Omega_i} d\Omega}, \tag{11}$$

where q, r belong to $L^2(\Omega)$, λ^* and λ are given by

$$\begin{aligned}\lambda &= \sup\{2k_v, 2(k_p+1), 2k_t+1\}, \quad \lambda^* \in \{0,1\} \cup S_{\lambda^*},\\ S_{\lambda^*} &= \begin{cases} (\text{dimensional unit of } h_i)^{-\lambda} & \text{if } h_i \text{ has dimension },\\ \emptyset & \text{if } h_i \text{ is dimensionless.}\end{cases}\end{aligned} \tag{12}$$

Due to the choice of the parameter λ, in the penalty bilinear form, the usual convergence rates will be maintained.

It is necessary to define the bilinear forms associated to the integrals on faces of elements. So, now we consider the parameters of stabilization defined as

$$\begin{aligned}&\beta^{i,l} = \beta^{i,*} \sup \left\{ \frac{\int_{\Gamma_i} h_i \left\|(G\nabla \mathbf{v}) \ : \mathbf{n}_i\right\|^2 d\Gamma}{\int_{\Omega_i} (G\nabla \mathbf{v}) \cdot (\nabla \mathbf{v}) d\Omega}; \quad \nabla \mathbf{v} \neq \mathbf{0}; \right.\\ &\left. \mathbf{v} \in ([H^1(\Omega_i)]^N \cap [P^{l,*}(\Omega_i)]^N) \right\}, \quad \beta^{i,l,t} = \beta^{i,*,t}\frac{\beta^{i,l}}{\beta^{i,*}},\\ &\beta^{i,*,t} \in (0, \beta^{i,*}], \quad \beta^{i,*} \geq \beta_0 > 0, \forall i,\end{aligned} \tag{13}$$

with $\mathbf{n}_i$ being the outward normal unit vector defined almost everywhere on Γ_i, $\beta^{i,*}$ and β_0 are dimensionless constants and the constant $\beta^{i,l}$ is independent of mesh parameters h_i, but depends on l.

Also, associated with a fixed face $e \in \mathcal{E}^{h,0}$, we consider for each $\Omega_i \in M^h$, the parameter

$$\beta^{i,e,l} = \begin{cases} 0 & \text{if} \quad meas(\Gamma_{i,e}) = 0,\\ \sup\{\beta^{i,l}, \beta^{j,l}\} & \text{if} \quad (\Gamma_i \cap \Gamma_j = e),\end{cases} \tag{14}$$

where $meas(\circ)$ denotes the Lebesgue positive measure.

Still, we consider the space $T(\Gamma \cup \Gamma_{int})$ and the broken space $H^{m,b}(\Omega)]^N$ defined by

$$\begin{aligned} T(\Gamma \cup \Gamma_{int}) &= \{\mathbf{r} \in [L^2(\Gamma \cup \Gamma_{int})]^N \ \text{such that there is}\\ &\quad\ \mathbf{w} \in [H^1(\Omega)]^N \ \text{and} \ \mathbf{w} = \mathbf{r} \ \text{on}\ \Gamma \cup \Gamma_{int}\},\\ [H^{m,b}(\Omega)]^N &= \{\mathbf{v} \in [L^2(\Omega)]^N \ \mathbf{v_i} \in [H^m(\Omega_i)]^N\}, \ (m \in \{1,2\}),\end{aligned} \tag{15}$$

and together with the stabilization parameters defined in (13), it is possible to introduce the bilinear forms defined on the boundary of Ω_i. For each $(\mathbf{w}, q, \mathbf{w}^t) \in [H^{2,b}(\Omega)]^N \times E_0^{1,p} \times T(\Gamma \cup \Gamma_{int})$ and $(\mathbf{v}, r, \mathbf{v}^t) \in [H^{2,b}(\Omega)]^N \times E_0^{1,p} \times T(\Gamma \cup \Gamma_{int})$ we define the following bilinear forms

$$\begin{aligned}\mathcal{Q}_0^i((\mathbf{w}, q, \mathbf{w}^t), (\mathbf{v}, r, \mathbf{v}^t)) &= \sum_{e \in \mathcal{E}^{h,0}} \int_{\Gamma_{i,e}} \frac{\beta^{i,e,l}}{h_{i,e}} (\mathbf{w}_i - \mathbf{w}_i^t) \cdot (\mathbf{v}_i - \mathbf{v}_i^t) d\Gamma\\ &+ \int_{\Gamma_i \cap \Gamma} \frac{\beta^{i,l}}{h_i} (\mathbf{w} \cdot \mathbf{v}) d\Gamma\end{aligned} \tag{16}$$

$$\mathcal{Q}_0^{i,t}((\mathbf{w}, q, \mathbf{w}^t), (\mathbf{v}, r, \mathbf{v}^t)) = \int_{\Gamma_i \cap \Gamma} \frac{\beta^{i,l,t}}{h_i} (\mathbf{w}_i - \mathbf{w}_i^t) \cdot (\mathbf{v} - \mathbf{v}^t) d\Gamma, \tag{17}$$

$$\mathcal{Q}_1^i((\mathbf{w},q,\mathbf{w}^t),(\mathbf{v},r,\mathbf{v}^t)) = \int_{\Gamma_i\cap\Gamma}(-((G\nabla\mathbf{w}_i)\,:\mathbf{n}_i)+q\mathbf{n})\cdot\mathbf{v}_i d\Gamma$$
$$+\sum_{e\in\mathcal{E}^{h,0}}\int_{\Gamma_{i,e}}(-((G\nabla\mathbf{w}_i)\,:\mathbf{n}_i)+q\mathbf{n}_i)\cdot(\mathbf{v}-\mathbf{v}^t)d\Gamma. \tag{18}$$

The bilinear form $\mathcal{Q}_0^{i,t}((\mathbf{w},q,\mathbf{w}^t),(\mathbf{v},r,\mathbf{v}^t))$, shown in Eq. (17), was presented in do Carmo et al. (2014). However, in the context of hybridized methods is the first time. It is important to mention that our formulation do not use the concepts of jumps, once the trace space is composed by continuous functions on $(\Gamma\cup\Gamma_i)$. Soon, for Ω_i and Ω_j such that $\Gamma_i\cap\Gamma_j=e$, where $e\in\mathcal{E}^{h,0}$, we must have $\mathbf{w}_i^t=\mathbf{w}_j^t$ in e.

In this manner, we can deduce the bilinear form associated with the process of hybridization via trace space continuous $\forall(\mathbf{w},q,\mathbf{w}^t)\in[H^{2,b}(\Omega)]^N\times E_0^{1,p}\times T(\Gamma_{int}\cup\Gamma)$ and $\forall(\mathbf{v},r,\mathbf{v}^t)\in[H^{2,b}(\Omega)]^N\times E_0^{1,p}\times T(\Gamma_{int}\cup\Gamma)$ as

$$a^{h,Hib}((\mathbf{w},q,\mathbf{w}^t),(\mathbf{v},r,\mathbf{v}^t)) = \sum_{i=1}^{Ne}\big(\mathcal{Q}_0^i((\mathbf{w},q,\mathbf{w}^t),(\mathbf{v},r,\mathbf{v}^t))$$
$$+\mathcal{Q}_0^{i,t}((\mathbf{w},q,\mathbf{w}^t),(\mathbf{v},r,\mathbf{v}^t))+\mathcal{Q}_1^i((\mathbf{w},q,\mathbf{w}^t),(\mathbf{v},r,\mathbf{v}^t))$$
$$-\mathcal{Q}_1^i((\mathbf{v},r,\mathbf{v}^t),(\mathbf{w},q,\mathbf{w}^t))\big), \tag{19}$$

wherein the negative sign indicates a hybridized continuous / discontinuous Galerkin formulation via trace space continuous with antisymmetric flux. Note that the Dirichlet conditions has been weakly imposed. This deduction is based on the last term of the equation (16), the first term of the equation (18) and from (19).

Now, for $(\mathbf{w},q)\in[H^{1,b}(\Omega)]^N\times E_0^{1,p}$ and $(\mathbf{v},r)\in[H^{1,b}(\Omega)]^N\times E_0^{1,p}$, the local bilinear forms associated to the differential operator are defined as

$$a_i(\mathbf{w},\mathbf{v}) = \int_{\Omega_i}G(\nabla\mathbf{w}_i)\cdot(\nabla\mathbf{v}_i)d\Omega \quad and \quad b_i(q,\mathbf{w}) = \int_{\Omega_i}q\,div(\mathbf{w}_i)d\Omega, \tag{20}$$

thus, the global bilinear form is given by

$$a^h((\mathbf{w},\mathbf{q}),(\mathbf{v},\mathbf{r})) = \sum_{i=1}^{N_e}(a_i(\mathbf{w},\mathbf{v})-b_i(q,\mathbf{v})+b_i(r,\mathbf{w})). \tag{21}$$

The bilinear form, for $(\mathbf{w},q,\mathbf{w}^t)\in[H^{2,b}(\Omega)]^N\times E_{p,0}^{1,d}\times T(\Gamma_{int}\cup\Gamma)$ and $(\mathbf{v},r,\mathbf{v}^t)\in[H^{2,b}(\Omega)]^N\times E_{p,0}^{1,d}\times T(\Gamma_{int}\cup\Gamma)$, is given by

$$A^{h,C_t-DG}((\mathbf{w},q,\mathbf{w}^t),(\mathbf{v},r,\mathbf{v}^t)) = a^h((\mathbf{w},q),(\mathbf{v},r))$$
$$+\ a^{h,Hib}((\mathbf{w},q,\mathbf{w}^t),(\mathbf{v},r,\mathbf{v}^t)), \tag{22}$$

where "C_t-DG" denotes the hybridized continuous / discontinuous Galerkin method via continuous trace space.

Now, the linear functionals of our formulation are defined as follow

$$\begin{aligned}
b_D(\mathbf{g},(\mathbf{v},r,\mathbf{v}^t)) &= \sum_{i=1}^{Ne}\int_{\Gamma_i\cap\Gamma}\left(\frac{\beta^{i,l}}{h_i}(\mathbf{g}\cdot\mathbf{v}_i)+(((G\nabla\mathbf{v}_i)\ :\mathbf{n}_i)\right.\\
&- \left. r\mathbf{n}_i)\cdot\mathbf{g}\right)d\Gamma,\\
b_0(\mathbf{f},(\mathbf{v},r,\mathbf{v}^t)) &= \sum_{i=1}^{Ne}\int_{\Omega_i}\mathbf{f}\cdot\mathbf{v}d\Omega, \qquad (23)\\
b^{h,C_t-DG}(\mathbf{v},r,\mathbf{v}^t)) &= b_D(\mathbf{g},(\mathbf{v},r,\mathbf{v}^t))+b_0(\mathbf{f},(\mathbf{v},r,\mathbf{v}^t)).
\end{aligned}$$

Finally, our hybridized continuous / discontinuous Galerkin formulation via trace space continuous, consists of finding $(\mathbf{u}^h,p^h,\mathbf{u}^{h,t})\in H^{h,k_v,N}\times P^{h,k_p}\times T^{h,k_t,N}$ satisfying the variational equation

$$\begin{aligned}
&A^{h,C_t-DG}((\mathbf{u}^h,p^h,\mathbf{u}^{h,t}),(\mathbf{v}^h,q^h,\mathbf{v}^{h,t}))+a^h_{proj}(p^h,q^h)+\overline{b}_p(p^h,q^h)\\
&=b^{h,C_t-DG}(\mathbf{v}^h,q^h,\mathbf{v}^{h,t}),\quad \forall(\mathbf{v}^h,q^h,\mathbf{v}^{h,t})\in H^{h,k_v,N}\times P^{h,k_p}\times T^{h,k_t,N}, \qquad (24)
\end{aligned}$$

with

$$a^h_{proj}(p^h,q^h)=\sum_{i=1}^{Ne}a^{h,i}_{proj}(p^h,q^h)\quad\text{and}\quad \overline{b}_p(p^h,q^h)=\sum_{i=1}^{Ne}\overline{b}^i_p(p^h,q^h), \qquad (25)$$

where $a^{h,i}_{proj}(p^h,q^h)$ is as given in (6) and $\overline{b}^i_p(p^h,q^h)$ is as given in (11).

4 NUMERICAL ANALYSIS OF THE FORMULATION

In this section, we describe some important results for the analysis of the proposed method. The complete demonstrations can be found in do Carmo et al. (submitted).

4.1 Consistence

We say that a method is consistent if it can replace the exact solution in the variational problem. Then, let $(\mathbf{u},p)\in[H^2(\Omega)]^N\times E_0^{1,p}$ be the exact solution of the problem model given by Eq. (1). For each Ω_i, we have

$$\left\{\begin{aligned}
-div(G\nabla\mathbf{u_i})+\nabla p_i &= \mathbf{f}\ \text{and}\ div(\mathbf{u_i})=0\ \text{a.e. in}\ \Omega_i,\\
\mathbf{u}_i &= \mathbf{g}\ \text{on}\ \Gamma_i\cap\Gamma\ \text{if}\ meas(\Gamma_i\cap\Gamma)>0,\\
\mathbf{u_i} &= \mathbf{u_j}=\mathbf{u^{t,exact}}\ \text{on}\ \Gamma_{ij}\ \text{if}\ meas(\Gamma_{ij})>0,\\
(G\nabla\mathbf{u_i}:\mathbf{n_i}-p_i\mathbf{n_i}) &= (G\nabla\mathbf{u_j}:\mathbf{n_i}-p_j\mathbf{n_i})\ \text{on}\ \Gamma_{ij}\ \text{if}\ meas(\Gamma_{ij})>0,
\end{aligned}\right. \qquad (26)$$

where $\mathbf{u^{t,exact}}$ is the trace of $\mathbf{u}$ on $(\Gamma_{int}\cup\Gamma)$.

The following result confirms the consistent:

Proposition 2. *The formulation defined in (22) is consistent in the sense that*

$$\begin{aligned}
A^{h,C_t-DG}((\mathbf{u},p,\mathbf{u^{t,exact}}),(\mathbf{v}^h,q^h,\mathbf{v}^{h,t}))&=b^{h,C_t-DG}(\mathbf{v}^h,q^h,\mathbf{v}^{h,t}),\\
&\forall(\mathbf{v}^h,q^h,\mathbf{v}^{h,t})\in H^{h,k_v,N}\times P^{h,k_p}\times T^{h,k_t,N}. \qquad (27)
\end{aligned}$$

Proof. The result is an immediate consequence of the equations given in (26), the Theorem of the divergence and the definition of $A^{h,C_t-DG}(\circ,\circ)$. □

4.2 Continuity, coercivity and convergence

The idea of this subsection is to show that the bilinear form of our formulation is continuous and weakly coercive (satisfies the $InfSup$ condition) in a suitable norm. In addition, we enunciate the error estimates.

In order to obtain this suitable norm, we introduce the functionals $J_0(\mathbf{v},q,\mathbf{v^t})$, $J_{0,k_v}(\mathbf{v},q,\mathbf{v^t})$ and $J_{1,k_v}(\mathbf{v},q,\mathbf{v^t})$ defined on $[H^{2,b}(\Omega)]^N \times E_0^{1,p} \times T(\Gamma_{int}\cup\Gamma)$ and the functional $J_1(\mathbf{v},q,\mathbf{v^t})$ defined on $H^{h,k_v,N} \times P^{h,k_p} \times T^{h,k_t,N}$ as follow

$$\begin{aligned}
J_0(\mathbf{v},q,\mathbf{v^t}) &= \sum_{i=1}^{N_e}\int_{\Omega_i}\left(G\left\|\nabla\mathbf{v}_i\right\|^2 + \frac{(h_i)^2}{\overline{G}_i}\left\|\nabla\hat{q}_i\right\|^2\right.\\
&+ \left.\frac{1}{\overline{G}_i}\left|\overline{q}_i\right|^2 + \frac{\lambda^*(h_i)^\lambda}{\overline{G}_i}\left|\overline{q}_i\right|^2\right)d\Omega,\\
J_1(\mathbf{v},q,\mathbf{v^t}) &= \sum_{i=1}^{N_e}\int_{\Omega_i}\left(\frac{(h_i)^2}{\overline{G}_i}\left\|\mathbf{Q}^i_{proj}(q)\right\|^2\right.\\
&+ \left.\frac{(h_i)^2}{\overline{G}_i}\left(\left\|\mathbf{Q}^i_{proj}(q)-\nabla q_i\right\|^2\right)\right)d\Omega,\\
J_{0,k_v}(\mathbf{v},q,\mathbf{v^t}) &= \sum_{i=1}^{N_e}\sum_{e\in\mathcal{E}^{h,0}}\int_{\Gamma_{i,e}}\frac{\beta^{i,e,k_v}}{h_{i,e}}\left\|\mathbf{v}_i-\mathbf{v}^t_i\right\|^2 d\Gamma,\\
J_{1,k_v}(\mathbf{v},q,\mathbf{v^t}) &= \sum_{i=1}^{N_e}\int_{\Gamma_i\cap\Gamma}\frac{\beta^{i,k_v}}{h_i}\left\|v_i\right\|^2 d\Gamma\\
&+ \int_{\Gamma_i\cap\Gamma}\frac{\beta^{i,k_v,t}}{h_i}\left\|\mathbf{v}_i-\mathbf{v}^t_i\right\|^2 d\Gamma.
\end{aligned} \tag{28}$$

The functionals defined in (28) together with the bilinear forms suggest on $H^{h,k_v,N}\times P^{h,k_p}\times T^{h,k_t,N}$ the following norm for the analysis of continuity and coercivity

$$\left\|(\mathbf{v},q,\mathbf{v^t})\right\|^2_{C_t-DG,k_v} = \sum_{i=0}^{1}\left(J_i(\mathbf{v},q,\mathbf{v^t}) + J_{i,k_v}(\mathbf{v},q,\mathbf{v^t})\right), \tag{29}$$

as well as suggest on $[H^{2,b}(\Omega)]^N \times E_0^{1,p} \times T(\Gamma_{int}\cup\Gamma)$ the norm

$$\left\|(\mathbf{v},q,\mathbf{v^t})\right\|^2_{C_t-DG,k_v,err} = J_0(\mathbf{v},q,\mathbf{v^t}) + \sum_{i=0}^{1}J_{i,k_v}(\mathbf{v},q,\mathbf{v^t}), \tag{30}$$

for the error estimates that will be presented.

With the purpose to prove the the continuity and weak coercivity, in the norm defined by the equation (29), it is necessary to define on $[H^{2,b}(\Omega)]^N \times E_0^{1,p} \times T(\Gamma_{int} \cup \Gamma)$ the functionals

$$
\begin{aligned}
J_{2,k_v}(\mathbf{v}, q, \mathbf{v^t}) &= \sum_{i=1}^{N_e} \sum_{e \in \mathcal{E}^{h,0}} \int_{\Gamma_{i,e}} \left(\frac{2\beta^{i,e,k_v}}{h_{i,e}} \left\| \mathbf{v}_i - \mathbf{v}_i^t \right\|^2 \right. \\
&+ \left. \frac{2h_{i,e}}{\beta^{i,e,k_v}} \left(\| G(\nabla \mathbf{v}_i) : \mathbf{n_i} \|^2 + \| q_i \, \mathbf{n_i} \|^2 \right) \right) d\Gamma, \\
J_{3,k_v}(\mathbf{v}, q, \mathbf{v^t}) &= \sum_{i=1}^{N_e} \int_{\Gamma_i \cap \Gamma} \left(\frac{2\beta^{i,k_v}}{h_i} \| \mathbf{v}_i \|^2 \right. \\
&+ \left. \frac{2h_i}{\beta^{i,k_v}} \left(\| G(\nabla \mathbf{v}_i) : \mathbf{n_i} \|^2 + \| q_i \, \mathbf{n_i} \|^2 \right) \right) d\Gamma, \qquad (31) \\
J_{4,k_v}(\mathbf{v}, q, \mathbf{v^t}) &= \sum_{i=1}^{N_e} \int_{\Gamma_i \cap \Gamma} \left(\frac{\beta^{i,k_v,t}}{h_i} \left\| \mathbf{v}_i - \mathbf{v}_i^t \right\|^2 \right) d\Gamma.
\end{aligned}
$$

Moreover, we introduce the classical inverse estimates evaluated in each Ω_i for $l \geq 1$ and given by

$$
\begin{aligned}
C^{i,0,l} &= \sup_{q \neq 0; q \in P^l(\Omega_i)} \frac{\int_{\Gamma_i \cap \Gamma} \frac{\overline{G_i} h_i}{\beta^{i,l}} |q|^2 d\Gamma + \sum_{e \in \mathcal{E}^{h,0}} \int_{\Gamma_{i,e}} \frac{\overline{G_i} h_{i,e}}{\beta^{i,e,l}} |q|^2 d\Gamma}{\int_{\Omega_i} |q|^2 d\Omega}, \\
C^{i,1,l} &= \sup_{v \neq 0; v \in P^l(\Omega_i)^N} \frac{2 \int_{\Gamma_i \cap \Gamma} \frac{\beta^{i,l}}{\overline{G_i} h_i} \| \mathbf{v} \|^2 d\Gamma + \sum_{e \in \mathcal{E}^{h,0}} \int_{\Gamma_{i,e}} \frac{\beta^{i,e,l}}{\overline{G_i} h_{i,e}} \| \mathbf{v} \|^2 d\Gamma}{\int_{\Omega_i} (h_i)^{-2} \| \mathbf{v} \|^2 d\Omega}, \\
C^{i,2,l} &= \sup_{v \neq 0; v \in P^l(\Omega_i)^N} \frac{\int_{\Omega_i} \frac{G}{\overline{G_i}} \| \nabla \mathbf{v} \|^2 d\Omega}{\int_{\Omega_i} (h_i)^{-2} \| \mathbf{v} \|^2 d\Omega}, \qquad (32)
\end{aligned}
$$

the identity and the inequality satisfying

$$
|ab| \leq \frac{\theta a^2}{2} + \frac{b^2}{2\theta}, \quad \text{and} \quad |ab| = \theta^* |a| \times \frac{|b|}{\theta^*}, \qquad (33)
$$

and still, we consider the following inequalities

$$
\begin{aligned}
\int_{\Omega_i} \overline{G_i} \, |div(\mathbf{v})|^2 d\Omega \leq N C_{vol,i} \int_{\Omega_i} G \, \| \nabla \mathbf{v} \|^2 d\Omega, \ \forall \mathbf{v} \in [H^1(\Omega)]^N, \\
C_{p,0}^i (h_i)^2 \int_{\Omega_i} \| \nabla \hat{q}_i \|^2 d\Omega \geq \int_{\Omega_i} |\hat{q}_i|^2 d\Omega, \ \forall q \in H^1(\Omega), \qquad (34)
\end{aligned}
$$

$$
C_{vol,i} = \sup \left\{ \frac{\overline{G_i}}{G(x)}; \ x \in \Omega_i \right\}; \quad C_{p,0}^i = \sup_{\hat{r}_i \neq 0; \hat{r}_i \in H^1(\Omega_i)} \left\{ \frac{\int_{\Omega_i} |\hat{r}_i|^2 d\Omega}{\int_{\Omega_i} (h_i)^2 \| \nabla \hat{r}_i \|^2 d\Omega} \right\},
$$

where $\hat{q}_i$ and $\hat{r}_i$ are functions with null mean in Ω_i.

Based on these previous definitions, we present a result that establishes the continuity of our formulation. This result is given by the following Lemma.

a) Continuity of "$A^{h,C_t-DG}(\circ,\circ) + a^h_{proj}(\circ,\circ) + \overline{b}_p(\circ,\circ)$"

Lemma 1. *There is a real constant $C_0 > 0$, such that for all $(\mathbf{w}, q, \mathbf{w}^t) \in H^{h,k_v,N} \times P^{h,k_p} \times$*

$T^{h,k_t,N}$ *and for all* $(\mathbf{v}, r, \mathbf{v}^t) \in H^{h,k_v,N} \times P^{h,k_p} \times T^{h,k_t,N}$

$$\left|A^{h,C_t-DG}((\mathbf{w}, q, \mathbf{w}^t), (\mathbf{v}, r, \mathbf{v}^t)) + a^h_{proj}(q, r) + \overline{b}_p(q, r)\right| \leq C_0 \left\|(\mathbf{w}, q, \mathbf{w}^t)\right\|_{C_t-DG,k_v} \left\|(\mathbf{v}, r, \mathbf{v}^t)\right\|_{C_t-DG,k_v}, \quad (35)$$

with $C^*_{p,0} = \max\{((1 + NC_{vol,i}), C^i_{p,0});\ i \in \{1, \cdots, Ne\}\}$.

Proof. The proof of this result can be found in do Carmo et al. (submitted). □

Now, we present two results that establish the weak coercivity of the bilinear form "$A^{h,C_t-DG}(\circ, \circ) + a^h_{proj}(\circ, \circ) + \overline{b}_p(\circ, \circ)$" in the norm defined by equation (29). These results are enunciated through the Lemma and Theorem below.

b) The weak coercivity of "$A^{h,C_t-DG}(\circ, \circ) + a^h_{proj}(\circ, \circ) + \overline{b}_p(\circ, \circ)$"

Lemma 2. *There is a real constant* $C_{IS} > 0$*, such that for all* $\mathbf{V} = (\mathbf{v}, q, \mathbf{v}^t) \in H^{h,k_v,N} \times P^{h,k_p} \times T^{h,k_t,N}$ *there exists* $\mathbf{W} = (\mathbf{w}, r, \mathbf{w}^t) \in H^{h,k_v,N} \times P^{h,k_p} \times T^{h,k_t,N}$ *dependent of* $\mathbf{V}$ *satisfying*

$$\begin{aligned} A^{h,C_t-DG}(\mathbf{V}, \mathbf{W}) &+ a^h_{proj}(q, r) + \overline{b}_p(q, r) \geq C_{IS} \|\mathbf{V}\|_{C_t-DG,k_v} \|\mathbf{W}\|_{C_t-DG,k_v}, \\ \mathbf{W} &= (1 - \omega)\mathbf{V} + \omega(\mathbf{V}^a + \mathbf{V}^b), \quad \omega \in (0, 1), \end{aligned} \quad (36)$$

with $\mathbf{V}^a = (\mathbf{v}^a, 0, \mathbf{v}^{a,t})$ *and* $\mathbf{V}^b = (\mathbf{v}^b, 0, 0)$ *belonging to* $H^{h,k_v,N} \times P^{h,k_p} \times T^{h,k_t,N}$.

Proof. The proof of Lemma 2 can be found in do Carmo et al. (submitted). □

Theorem 1. *There exists a real constant* $C_{IS} > 0$ *independent of the mesh parameters such that*

$$\inf \left\{ \sup \left\{ \frac{A^{h,C_t-DG}(\mathbf{V}^a, \mathbf{V}^b) + a^h_{proj}(q, r) + \overline{b}_p(q, r)}{\|\mathbf{V}^a\|_{C_t-DG,k_v} \|\mathbf{V}^b\|_{C_t-DG,k_v}}; \right. \right.$$
$$\left. \mathbf{V}^b = (\mathbf{w}, q, \mathbf{w}^t) \neq \mathbf{0};\ \mathbf{V}^b \in H^{h,k_v,N} \times P^{h,k_p} \times T^{h,k_t,N} \right\}; \quad (37)$$
$$\left. \mathbf{V}^a = (\mathbf{v}, r, \mathbf{v}^t) \neq \mathbf{0};\ \mathbf{V}^a \in H^{h,k_v,N} \times P^{h,k_p} \times T^{h,k_t,N} \right\} \geq C_{IS}.$$

with $C_{IS} = \frac{\omega\omega_0}{(1-\omega)+\omega(C_{vd,a}+(C_{B,1})^{1/2})}$.

Proof. The proof of this Theorem follows directly from Lemma 2, defining C_{IS} as above. □

Theorem 2. *The variational problem defined in (22) is well posed in the sense that the solution exists and is unique.*

Proof. The result follows the fact that the linear functional given by (23) is continuous, the bilinear forms are continuous and weakly coercive and, therefore, is a direct consequence of the *Nečas* Theorem given in Ern & Guermond (2004). □

4.3 Convergence properties of the approximate solution

We consider the following error functions

$$\begin{aligned} \mathcal{E}^h &= (\mathbf{u}^h - \mathbf{u}, p^h - p, \mathbf{u}^t - \mathbf{u}^{t,exact}), \\ \mathcal{E}^{h,I} &= (\mathbf{u}^{h,I} - \mathbf{u}, p^{h,I} - p, \mathbf{u}^{h,t,I} - \mathbf{u}^{t,exact}), \\ \mathcal{E}^{h,h,I} &= (\mathbf{u}^h - \mathbf{u}^{h,I}, p^h - p^{h,I}, \mathbf{u}^{h,t} - \mathbf{u}^{h,t,I}), \end{aligned} \tag{38}$$

with $(\mathbf{u}, p) \in \left([(H^{k_v+1}(\Omega)]^N \cap [C^0(\Omega \cup \Gamma)]^N\right) \times (H^{k_p+1}(\Omega) \ \cap C^0(\Omega \cup \Gamma))$ as being the exact solution of the problem defined in (1), $\mathbf{u}^{t,exact}$ as being the trace of $\mathbf{u}$ in $(\Gamma_{int} \cup \Gamma)$, $(\mathbf{u}^{h,I}, p^{h,I}, \mathbf{u}^{h,t,I})$ the usual interpolant of $(\mathbf{u}, p, \mathbf{u}^{t,exact})$ and $(\mathbf{u}^h, p^h, \mathbf{u}^{h,t})$ the solution of the variational problem defined by (22).

From (38) and the properties of approximation of P^{h,k_p} we obtain

$$\begin{aligned} \mathcal{E}^h &= \mathcal{E}^{h,I} + \mathcal{E}^{h,h,I}, \\ \left\| p_i^{h,I} \right\|^2_{H^{(k_p+1)}(\Omega_i)} &\leq C_*^{d,P} \left\| p_i \right\|^2_{H^{(k_p+1)}(\Omega_i)} \ \forall \Omega_i. \end{aligned} \tag{39}$$

Lemma 3. *The solution* $(\mathbf{u}^h, p^h, \mathbf{u}^{h,t})$ *converges to the interpolant* $(\mathbf{u}^{h,I}, p^{h,I}, \mathbf{u}^{h,t,I})$ *with the following convergence rate*

$$\begin{aligned} &\left\| \mathcal{E}^{h,h,I} \right\|_{C_t-DG,k_v,err} \leq \left\| \mathcal{E}^{h,h,I} \right\|_{C_t-DG,k_v} \leq \frac{1}{C_{IS}} \left(\left(\sum_{i=1}^{N_e} N C_i^{P,0} C_*^{d,P} \frac{\rho_{i,1}}{\overline{G_i}} \right.\right. \\ &\left. \times (h_i)^{2(k_{vp}+1)} \left\| p_i \right\|^2_{H^{(k_p+1)}(\Omega_i)} \right)^{1/2} + \big(3 \left(1 + 2(C_{2,k_v})^2 + \right. \\ &\left. (\rho_{1,max}+1)^2 + 1 + (1 + C_{p,0}^*)^2 \right)\big)^{1/2} \times \left(J_0(\mathcal{E}^{h,I}) + \sum_{l=0}^{1} J_{l,k_v}(\mathcal{E}^{h,I}) \right)^{1/2} \\ &\left. + \left(\sum_{i=1}^{N_e} \lambda^* C_*^{d,P} (h_i)^{\lambda} \left\| p_i \right\|^2_{H^{(k_p+1)}(\Omega_i)} \right)^{1/2} \right), \end{aligned} \tag{40}$$

where λ^* *and* λ *are as given in (12) and* $k_{vp} = \inf\{k_v, k_p\}$.

Proof. The proof of this Theorem can be found in do Carmo et al. (submitted). ☐

Lemma 4. *The solution* $(\mathbf{u}^h, p^h, \mathbf{u}^{h,t})$ *converges to the exact solution* $(\mathbf{u}, p, \mathbf{u}^{t,exact})$ *with the following well-established convergence rate*

$$\left\| \mathcal{E}^h \right\|_{C_t-DG,k_v,err} \leq \left\| \mathcal{E}^{h,I} \right\|_{C_t-DG,k_v,err} + \left\| \mathcal{E}^{h,h,I} \right\|_{C_t-DG,k_v,err}. \tag{41}$$

Proof. From equations given in (38), the triangular inequality and Lemma 3, the result follows immediately. ☐

5 NUMERICAL EXPERIMENTS

In this section several numerical experiments are presented in order to verify the accuracy and robustness of the $C_t - DG$ method developed in this paper.

All the numerical experiments were performed using triangular meshes, wherein each side of a square domain was uniformly discretized with 10, 20, 30, 40, 50, 60, and 70 partitions, for obtaining meshes nearly regular. The value $\beta^{i,*} = 25$ was chosen because it allows an adequate capture of the singularities of pressure on the corners of the mesh as well as leads to a solution with the best properties of robustness for problems with smooth solution. Also, we adopted the viscosity $G = 1$ in our simulations.

We use interpolation $P2-P1-P2$ for the velocity, pressure and trace variable, respectively, for the $C_t - DG$, the one presented in do Carmo et al. (2015) and the $C_t - DG*$ methods. It is important to mention that the $C_t - DG*$ method is our method without using the Eq. (17), using only the Dirichlet conditions imposed strongly in the space $T^{h,k_t,N}$. Although the $C_t - DG*$ method does not use the Eq. (17), its computational cost is the same order of the $C_t - DG$ method. However, the $C_t - DG$ method has the best robustness due to the inclusion of this equation, as will be seen in the following experiments. We also include the classical continuous Galerkin method in our numerical experiments.

As previously mentioned, one of the advantages of our formulation is the reduction of the number of degrees of freedom in relation to the usual hybridized methods. The degrees of freedom of $C_t - DG$ and $C_t - DG*$ methods are associated only with the velocity, i.e, the constant component as well as the null mean component are eliminated completely. These components are not eliminated in the do Carmo et al. (2015) and Galerkin methods.

We must call the attention that, even that the results presented here just use interpolation $P2 - P1 - P2$, the polynomial degree for the pressure can assume any value equal or higher than zero, as long as the polynomial degree for the velocity and the space trace are equal or higher than two. This conclusion is deduced through the Lemmas and Theorems mentioned before and from definition of spaces in Eq. (3).

The numerical experiments are divided into two kinds. The first, the cavity problem, has as goal to verify the performance of the four methods mentioned previously for capturing singularity of pressure on the corners of the mesh. The second type is divide in two problems with smooth solution. In the first problem the pressure is null on the boundary of the domain and for the second the pressure is not null on two faces of the boundary of the domain. These two choices have the objective of verifying the robustness of the four methods to obtain the pressure on the boundary.

5.1 Experiment 1: the cavity problem

The cavity problem is modeled by

$$\begin{aligned} &-div(\nabla\mathbf{u}) + \nabla p = 0 \quad \text{and} \quad div(\mathbf{u}) = 0 \quad \text{a.e in } \Omega, \\ u_1 &= 0 \quad \text{on} \quad \bigcup_{m=1}^{4} \Gamma_m \text{ and } \quad u_2 = 0 \quad \text{on} \quad \Gamma_1 \cup \Gamma_3 \cup \Gamma_4, \\ u_2 &= 1 \quad \text{on} \quad \{(0.5, y);\ -0.5 < y < 0.5\}, \end{aligned} \tag{42}$$

with $\Omega = (-0.5, 0.5) \times (-0.5, 0.5)$, $\Gamma_1 = \{(-0.5, y); -0.5 \leq y \leq 0.5\}$, $\Gamma_2 = \{(0.5, y); -0.5 \leq y \leq 0.5\}$, $\Gamma_3 = \{(x, -0.5); -0.5 \leq x \leq 0.5\}$ and $\Gamma_4 = \{(x, 0.5); -0.5 \leq x \leq 0.5\}$.

In order to obtain the graphs that permit a sensitivity analysis for the singularities of the pressure, we normalize the pressure using the *PMF (Pressure Multiplication Factor)*, which represents the maximum value of the module of pressure. Therefore, for each graph that represents the elevation of the pressure, we must multiply the value given in the graph by the respective value of the PMF that is associated to the graph.

The elevation of the pressure normalized through the correspondent PMF is presented in Figure 1 (right side) for the $C_t - DG$ method. In the table of Figure 1 are presented the PMF for the four methods analyzed. We observe that the $C_t - DG*$ method has an ability slightly better for capturing the singularities. In addition, we note greater ability of the methods $C_t - DG$, $C_t - DG*$ and do Carmo et al. (2015) to capture the singularities of the pressure on the corners than of the Galerkin method.

Method	PMF
$C_t - DG$	1313.38
do Carmo et al. (2015)	1231.75
$C_t - DG*$	1361.08
Galerkin	1179.55

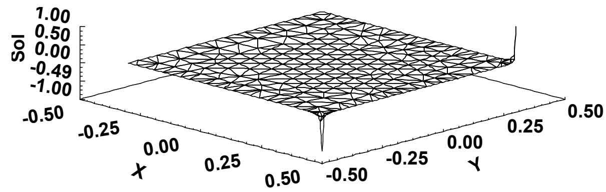

Figure 1: Ability to capture singularities.

In Figure 2 we present the results for the discontinuous velocity. It must observed that the four methods have equivalent behavior.

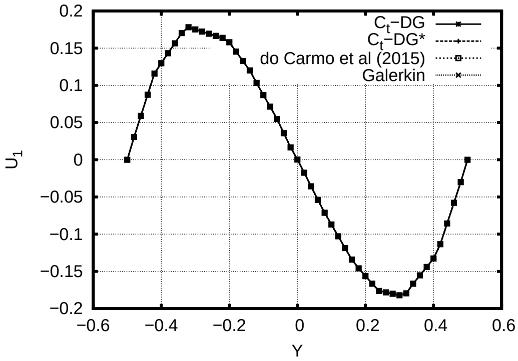

(a) Component of velocity $u_1^h = U_1; y = Y$

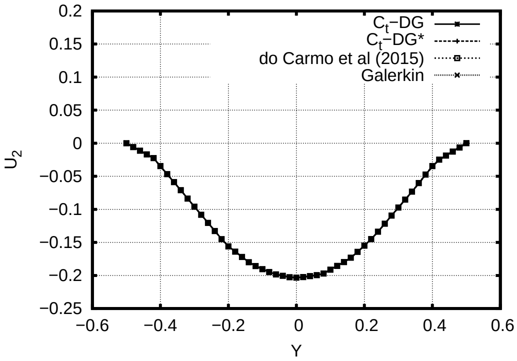

(b) Component of velocity $u_2^h = U_2; y = Y$

Figure 2: Components of velocity u_1^h and u_2^h on section $x = 0$.

5.2 Experiment 2: smooth solutions

Following Donea & Huerta (2003), we consider the Stokes problem on the square $\Omega = (0, 1) \times (0, 1)$ and Γ being the boundary of Ω

$$-div(\nabla \mathbf{u}) + \nabla p = \mathbf{f} \quad \text{and} \quad div(\mathbf{u}) = 0 \ \text{ in } \Omega \quad \text{and} \quad \mathbf{u} = \mathbf{0} \ \text{ on } \Gamma, \tag{43}$$

with a known analytic solution given by

$$u_1 = x^2(1-x)^2(2y - 6y^2 + 4y^3), \quad u_2 = -y^2(1-y)^2(2x - 6x^2 + 4x^3)$$
$$p = \sin(\pi x)\sin(\pi y) - \frac{4}{\pi^2}. \tag{44}$$

The components of $\mathbf{f}$ are given by:

$$
\begin{aligned}
f_1 &= (12-24y)x^4 + (-24+48y)x^3 + (-48y+72y^2-48y^3+12)x^2 \\
&+ (-2+24y-72y^2+48y^3)x + 1 - 4y + 12y^2 - 8y^3 - (1-2x) \\
&+ \pi\cos(\pi x)\sin(\pi y) \qquad (45)\\
f_2 &= (8-48y+48y^2)x^3 + (-12+72y-72y^2)x^2 + (4-24y+48y^2 \\
&- 48y^3+24y^4)x - 12y^2 + 24y^3 - 12y^4 + \pi\sin(\pi x)\cos(\pi y).
\end{aligned}
$$

The analytic solution described previously was used to compute the errors presented in Figure 3. We exhibit the error for the velocity and for the divergent of the velocity in the $L^2(\Omega)$ norm. Also, we exhibit the error in the H^1 seminorm for the velocity.

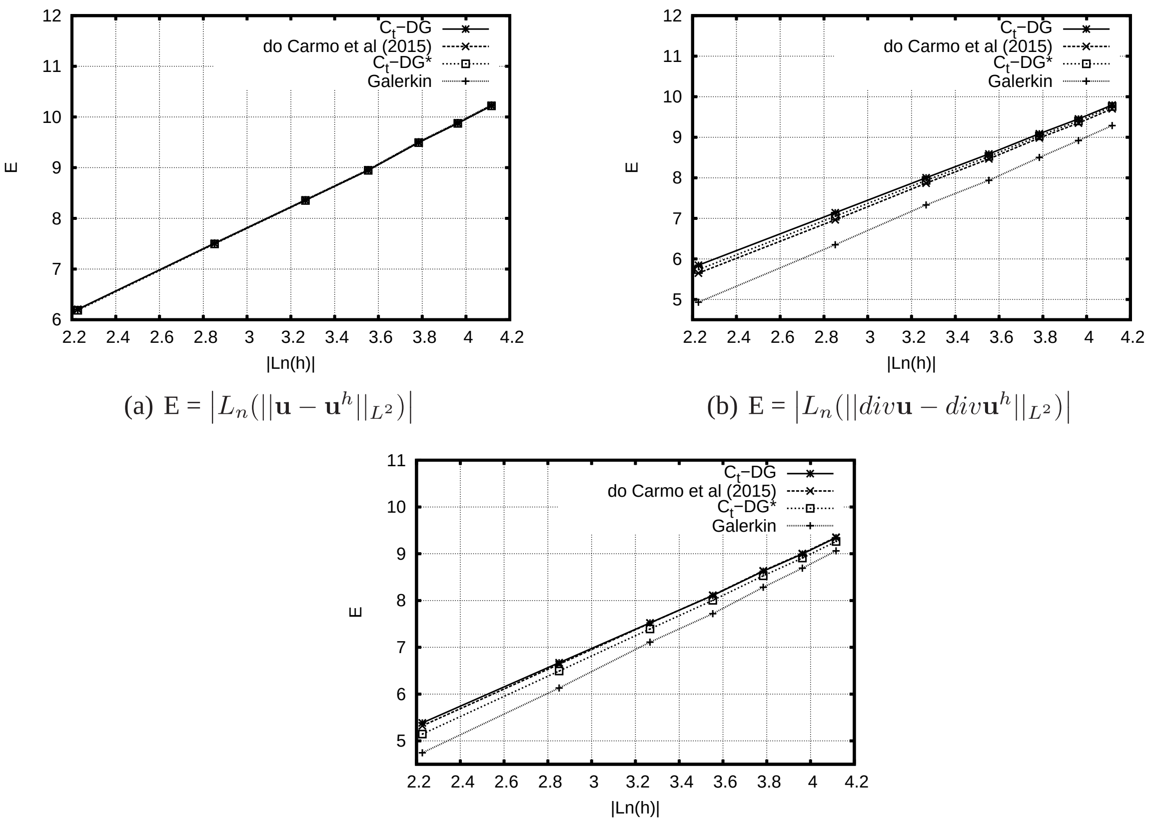

(a) E = $\left|L_n(||\mathbf{u}-\mathbf{u}^h||_{L^2})\right|$

(b) E = $\left|L_n(||div\mathbf{u}-div\mathbf{u}^h||_{L^2})\right|$

(c) E = $\left|L_n(|\mathbf{u}-\mathbf{u}^h|_{H^1})\right|$

Figure 3: (Module of L_n of error) $\times\,|L_n(h)|$**.**

As can be seen in Figure 3(a) it is possible infer that the error of the velocity in the $L^2(\Omega)$ norm for all the methods are equivalent, i.e, they have the same accuracy. On the other hand, in Figure 3(b) the $C_t - DG$ method provides an accuracy slightly better in the $L^2(\Omega)$ norm when compared with the do Carmo et al. (2015) and $C_t - DG*$ methods for the divergent of the velocity and, therefore, a better representation of the incompressibility of the velocity field. From Figure 3(c) we observe that the method presented in this paper has accuracy slightly better for the velocity in the H^1 seminorm than the other three studied methods. However, all the methods have the same convergence rates.

Finally, we can deduce from the graphs presented that the Galerkin method has the smaller accuracy and that the other methods present an excess of convergence in relation to the Galerkin method.

It is important to observe that the graphs presented in Figure 3(c) are approximately parallel straight lines, indicating that the four methods have equivalent convergence rates, including the Galerkin method. Due to this fact, we present in Figure 4 the convergence rates only for the $C_t - DG$ method.

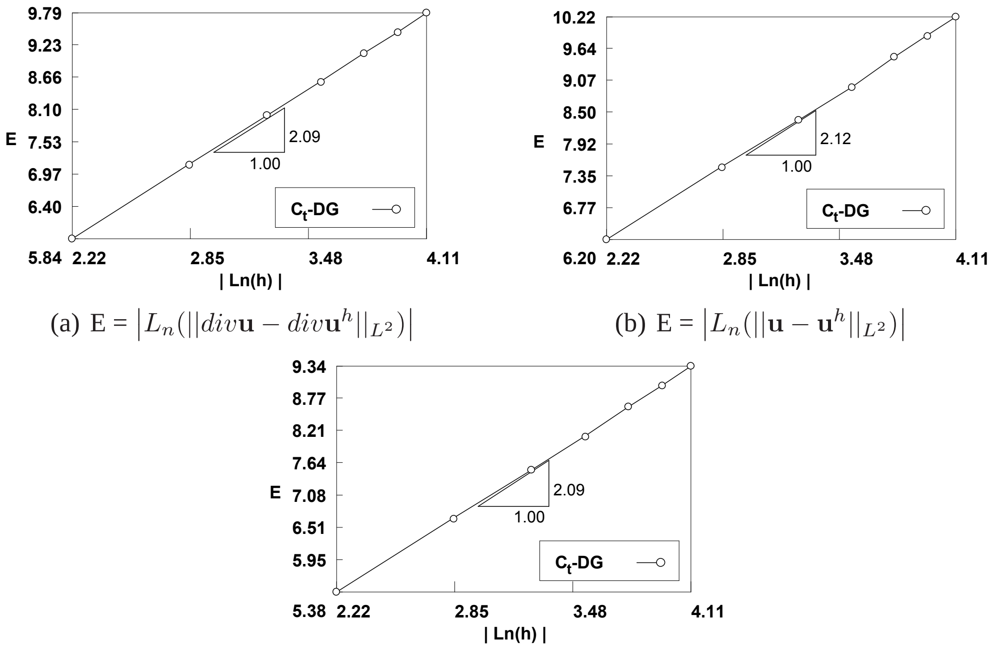

(a) E = $\left|L_n(||div\mathbf{u} - div\mathbf{u}^h||_{L^2})\right|$ (b) E = $\left|L_n(||\mathbf{u} - \mathbf{u}^h||_{L^2})\right|$

(c) E = $\left|L_n(|\mathbf{u} - \mathbf{u}^h|_{H^1})\right|$

Figure 4: Convergence rates for $C_t - DG$ method.

From Figure 4(a) we conclude that the convergence rate in the norm $L^2(\Omega)$ is optimal for the divergent of the velocity $(O((h_{mean})^{k_v}))$. In the Figure 4(b) we can observe that the convergence rate is suboptimal for the velocity $(O((h_{mean})^{k_v}))$ in the norm $L^2(\Omega)$. Notice that in the Figure 4(c) the convergence rate for velocity in the semi norm $[H^1(\Omega)]^N$ is optimal $(O((h_{mean})^{k_v}))$.

The Dirichlet conditions weakly imposed does not allow us to obtain the optimal convergence rate in the norm $L^2(\Omega)$ for the velocity. Also, it is well known that the symmetric formulation results in suboptimal in the norm $L^2(\Omega)$ for the velocity if we use even degree polynomials.

In Table 1 we compare the accuracy of the pressure in $L^2(\Omega)$ norm for the simulated methods. From Table 1 we can infer that, for the pressure, the most accurate solution was obtained with the $C_t - DG$ method, followed by the $C_t - DG*$ method.

Table 1: Accuracy of the pressure for the methods using $\frac{\|p-p^h\|_{L^2}}{(h_{mean})^2\|p\|_{H^2}}$.

h_{mean}	$C_t - DG*$	Galerkin	$C_t - DG$	CARMO *et al.*(2015)
0.10789	4.91273	6.03328	3.46292	6.31028
0.05775	2.71630	6.98783	2.80741	5.88636
0.03814	5.17891	8.20402	4.27345	6.90431
0.02862	4.91740	8.06011	3.35187	6.31424
0.02274	3.57151	4.73772	2.92005	4.89807
0.01901	5.02347	7.81667	2.50352	6.77887
0.01630	3.36633	4.74439	1.80752	4.84615

In Figure 5, we present the elevation of the pressure for the $C_t - DG$ method (right side). The exact value of pressure in $(0.5, 0.5) = 1.0000$. Notice that, in the table of Figure 5, the $C_t - DG$ method is more accurate to obtain the pressure than the others. However, the other three methods can be considered as having a similar performance.

Method	Sol p^h
$C_t - DG$	1.0005
do Carmo et al. (2015)	1.0020
$C_t - DG*$	1.0011
Galerkin	0.9962

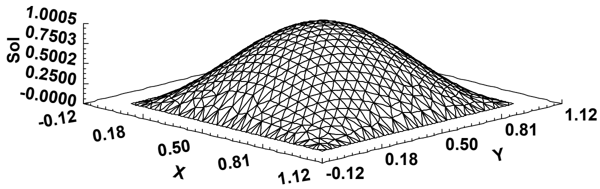

Figure 5: Elevations of the pressure p^h = Sol.

For the domain defined by $\Omega = (0, 1) \times (0, 1)$ where Γ is the boundary of Ω, consider the following problem

$$-div(\nabla \mathbf{u}) + \nabla p = \mathbf{f} \quad and \quad div(\mathbf{u}) = 0 \text{ in } \Omega \text{ and } \quad \mathbf{u} = \mathbf{0} \text{ on } \Gamma, \tag{46}$$

with the components of $\mathbf{f}$ being given as follow

$$\begin{aligned} f_1 &= (12 - 24y)x^4 + (-24 + 48y)x^3 + (-48y + 72y^2 - 48y^3 + 12)x^2 \\ &+ (-2 + 24y - 72y^2 + 48y^3)x + 1 - 4y + 12y^2 - 8y^3 \\ f_2 &= (8 - 48y + 48y^2)x^3 + (-12 + 72y - 72y^2)x^2 + (4 - 24y + 48y^2 \\ &- 48y^3 + 24y^4)x - 12y^2 + 24y^3 - 12y^4. \end{aligned} \tag{47}$$

The exact solution of this problem is given as follows

$$\begin{aligned} u_1 &= x^2(1 - x)^2(2y - 6y^2 + 4y^3), \quad u_2 = -y^2(1 - y)^2(2x - 6x^2 + 4x^3) \\ p &= x(1 - x) - \frac{1}{6}. \end{aligned} \tag{48}$$

The elevations of the pressure obtained with the $C_t - DG$ method (right side) are presented in Figure 6. The exact value of pressure in $(0.5, 0.5) = 0.25000$. In the table of Figure 6 is presented the approximate solution of the pressure for the four methods analyzed. We can observe that the $C_t - DG$ method showed a better performance in relation to the other methods for determining the maximum elevation.

Method	Sol p^h
$C_t - DG$	0.25000
do Carmo et al. (2015)	0.25066
$C_t - DG*$	0.25196
Galerkin	0.25055

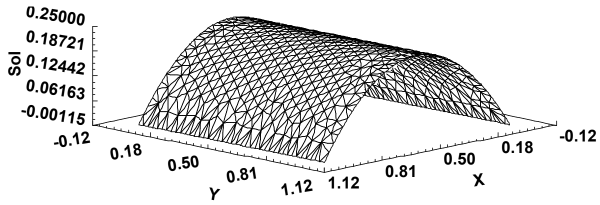

Figure 6: Elevations of the pressure p^h = Sol.

We end this numerical experiment presenting in Figure 7 the graphs for the pressure evaluated on section $y = 0$ for the four methods studied, together with the exact solution.

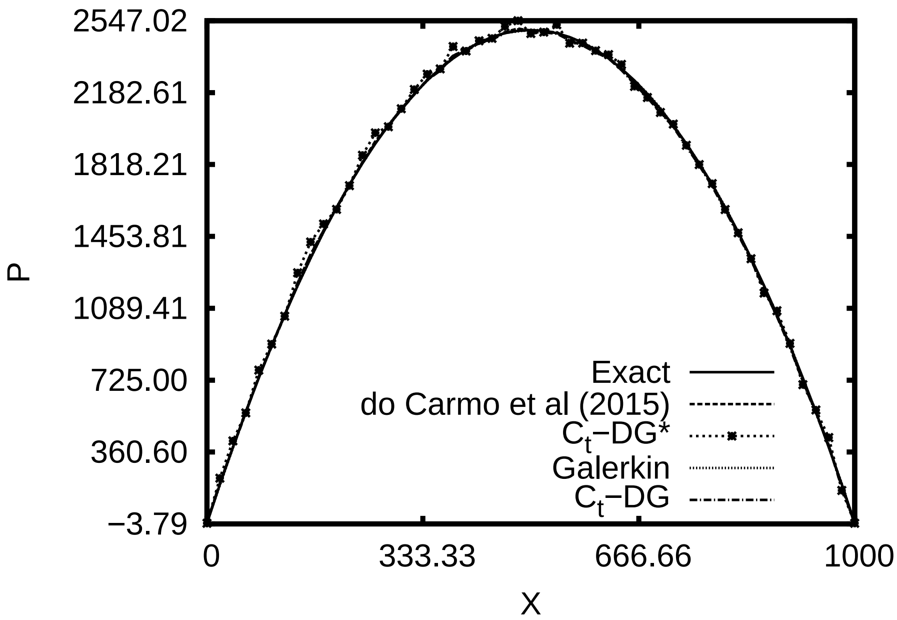

(a) 10^4Pressure=P; 10^3 x=W; on section $y = 0$

Figure 7: Pressure for the four methods and the exact solution.

We can observe that the $C_t - DG$ method, the Galerkin method and the do Carmo et al. (2015) method agree very well with the exact solution. However, the $C_t - DG*$ method presents small oscillations when compared with the exact solution. We conjecture that the lack of the bilinear form given in (17) together with fact that this method uses strong Dirichlet condition for the component of trace space are the causes of this.

6 CONCLUSIONS

In this paper, we developed a hybridized continuous / discontinuous Galerkin formulation via continuous trace space applied for the Stokes problem. As previously mentioned, one of the differentials of our formulation is the penalty bilinear form. This formulation was presented in order to perform a full static condensation of pressure at element level, i.e, the constant component as well as the null mean component are eliminated completely. Moreover, it was introduced in order to not change the usual convergence rates.

In order to verify the proposed methodology, we presented the numerical results with the goal to confirm the convergence rates, the robustness and accuracy of the proposed formulation. A satisfactory agreement was observed between the numerical results and the analytical solution. It must observed that the $C_t - DG*$ method showed an ability approximately 3.53 percent better than the $C_t - DG$ method for capturing singularities of pressure on the corners, i.e, these methods were quasi equivalent in what singularities capture is concerned. However, for the other methods used in the comparison, the $C_t - DG$ method presented the better ability for capturing the singularities of the pressure for the cavity problem. The second case was the problems with smooth solution. For this case, the $C_t - DG$ method presented the best performance in relation to the other methods.

Acknowledgements

The authors acknowledge the financial support of CNPQ projects 301174 / 2012-1 and 306933 / 2014-4 as well as of CAPES for their support to the development of this work.

REFERENCES

Adams, R. A. (1975). *Sobolev Spaces*. New York: Academic Press.

Arnold, D. N., Brezzi, F., Cockburn, B., & Marini, L. D. (2001). Unified analysis of discontinuous galerkin methods for elliptic problems. *SIAM J. Numer. Anal.*, *39*, 1749–1779.

Baumann, C. E., & Oden, J. T. (1999). A discontinuous hp finite element method for convectiondiffusion problems. *Computer Methods in Applied Mechanics and Engineering*, *175*, 311 – 341.

do Carmo, E. G. D., & Duarte, A. V. C. (2000). A discontinuous finite element-based domain decomposition method. *Computer Methods in Applied Mechanics and Engineering*, *190*, 825 – 843.

do Carmo, E. G. D., Fernandes, K. P., & Mansur, W. J. (submitted). A hybridized continuous / discontinuous galerkin formulation for stokes problem with minimum global system. *Computational and Applied Mathematics (submitted)*, .

do Carmo, E. G. D., Fernandes, M. A., & Mansur, W. J. (2015). Continuous/discontinuous galerkin methods stabilized through transfer functions applied to the incompressible elasticity and to the stokes problem. *Computer Methods in Applied Mechanics and Engineering*, *283*, 806 – 840.

do Carmo, E. G. D., Fernandes, M. T. C. A., & Mansur, W. J. (2014). Continuous/discontinuous galerkin methods applied to elasticity problems. *Computer Methods in Applied Mechanics and Engineering*, *269*, 291 – 314.

Cockburn, B., Kanschat, G., & Schotzau, D. (2005). A locally conservative ldg method for the incompressible navier-stokes equation. *Mathematics of Computation*, *74*, 1067 – 1095.

Cockburn, B., Nguyen, J. G. N., Peraire, J., & Sayas, F. (2011). Analysis of hdg methods for stokes flow. *Mathematics of Computation*, *80*, 723 – 760.

Donea, J., & Huerta, A. (2003). *Finite Element Methods for Flow Problems*. (1st ed.). Wiley.

Egger, H., & Waluga, C. (2013). hp analysis of a hybrid dg method for stokes flow. *IMA Journal of Numerical Analysis*, (pp. 687–721).

Ern, A., & Guermond, J.-L. (2004). *Theory and Practice of Finite Elements*. (1st ed.). New York: Springer.

Fortin, M. (1981). Old and new finite elements for incompressible flows. *International Journal for Numerical Methods in Fluids*, *1*, 347–364.

Hughes, T. J., Scovazzi, G., Bochev, P. B., & Buffa, A. (2006). A multiscale discontinuous galerkin method with the computational structure of a continuous galerkin method. *Computer Methods in Applied Mechanics and Engineering*, *195*, 2761 – 2787.

Nguyen, N., Peraire, J., & Cockburn, B. (2010). A hybridizable discontinuous galerkin method for stokes flow. *Computer Methods in Applied Mechanics and Engineering*, *199*, 582 – 597.

Reed, W. H., & Hill, T. R. (1973). Triangular mesh methods for the neutron transport equation. *Los Alamos Scientific Laboratory*, .